Front. Optoelectron. 2017, 10(4): 370–377
DOI 10.1007/s12200-017-0705-9

RESEARCH ARTICLE

Design and simulation to improve the structural efficiency of green light emission of GaN/InGaN/AlGaN light emitting diode

Sakhawat HUSSAIN (✉), Tasnim ZERIN, Md. Ashik KHAN

Department of Electrical and Electronic Engineering, University of Dhaka, Dhaka-1000, Bangladesh

Abstract This study considered the design of an efficient, high brightness polar InGaN/GaN light emitting diode (LED) structure with AlGaN capping layer for green light emission. The deposition of high In ($>15\%$) composition within InGaN quantum well (QW) has limitations when providing intense green light. To design an effective model for a highly efficient InGaN green LEDs, this study considered the compositions of indium and aluminum for $In_xGa_{1-x}N$ QW and $Al_yGa_{1-y}N$ cap layers, along with different layer thicknesses of well, barrier and cap. These structural properties significantly affect different properties. For example, these properties affect electric fields of layers, polarization, overall elastic stress energy and lattice parameter of the structure, emission wavelength, and intensity of the emitted light. Three models with different composition and layer thicknesses are simulated and analyzed to obtain green light with in-plane equilibrium lattice parameter close to GaN (3.189 Å) with the highest oscillator strength values. A structure model is obtained with an oscillator strength value of 1.18×10^{-1} and least in-plane equilibrium lattice constant of 3.218 Å. This emitter can emit at a wavelength of 540 nm, which is the expected design for the fabrication of highly efficient, bright green LEDs.

Keywords green light emitting diode (LED), lattice parameter, oscillator strength, InGaN quantum well (QW), AlGaN capping layer

1 Introduction

Group III-Nitride-based light emitting diodes (LEDs) are important in attaining high external quantum efficiency in the blue wavelength range of visible spectrum [1–3]. However, the quantum efficiency of $In_xGa_{1-x}N$/GaN quantum wells (QWs) strongly decreases [2,4] for longer wavelengths that correspond to green and yellowish green (525–565 nm) colors. The degradation of optical properties is mainly attributed to the increase of In composition in $In_xGa_{1-x}N$ QWs [5]. Growth temperature should be decreased to favor large In incorporation in GaN, which can lead to an increase in extended defects or point defects density. Increased In composition within QWs induces an increased stress in the structure. Risk of defect formation, such as V-defects or misfit dislocations, occurs [6] if stress is excessively high. However, growth processes for In-rich ($In>20\%$) QWs affect the In fluctuation, carrier localization, as well as the strain relaxation processes of the structure; these mechanisms affect the structural and optical properties of the device [7–9]. The reduced oscillator strength of the fundamental transition of QW attributed to internal piezo-electric field (quantum confined Stark effect) becomes increasingly pronounced for QWs grown along the *c*-plane. To compensate for the effect of strain, a number of research groups used the growth of GaN on nonpolar or semipolar substrates [10,11], thick InGaN templates [12], and quantum dot structures [13]. This approach was used to demonstrate green lasers and yellow emitting LEDs [14,15]. However, to obtain the same emission wavelength, the In composition in $In_xGa_{1-x}N$ QWs grown along a semi-polar orientation should be larger than that for the polar orientation [16].

The optical properties of conventional polar growth (*c*-plane) systems can be improved by using staggered InGaN structures [17,18], screening the internal electric field by

Received February 20, 2017; accepted June 21, 2017

E-mail: sakhawat@du.ac.bd

doping into a multiple quantum well (MQW) [19], and using strain-compensated $Al_yGa_{1-y}N$ inter-layers as $Al_yGa_{1-y}N$ layers tensely strained on GaN [20]. Replacing part of the GaN barrier layer by a ternary alloy can increase the magnitude of in-plane potential fluctuations, thereby strengthening carrier localization [21]. Thus, $Al_yGa_{1-y}N$ effectively reduces the total strain energy of MQW [22,23]. InGaN/AlGaN MQW improves the external quantum efficiency and increases the photoluminescence (PL) intensity [24]. The use of a thin $Al_yGa_{1-y}N$ layer helps improve the PL intensity of $In_xGa_{1-x}N$ single QW when its emission wavelength increases [25]. The most significant result is the presence of green to red LEDs grown by metal oxide chemical vapor deposition (MOCVD) with high external quantum efficiency at this wavelength range [20,26–28]. The construction of efficient green to red LEDs are important in achieving monolithic white LEDs because they can act as light converters in the structure [29–31].

In this study, we aim to identify the best GaN/$In_xGa_{1-x}N$/$Al_yGa_{1-y}N$ structure to obtain the highest force of oscillator or oscillator strength values, which in turn corresponds to PL, for green light (525–565 nm) emission. When searching for such high oscillator strength value, we calculated and sought the lowest overall strain energy of the structure because obtaining the minimum strain energy value to minimize the chance of defect in the structure is an obvious approach. Finally, we aimed to explain and justify the results obtained to propose the best structure for green light emission.

2 Theoretical background for modeling

Room temperature e1-hh1 transition energy for polar (*c*-plane) GaN/$In_xGa_{1-x}N$/$Al_yGa_{1-y}N$ structures was calculated by solving the Schrödinger equation via envelop function formalism. This calculation is shown in Fig. 1 as a function of the QW thickness (L_W) and In composition [32]. The figure shows the possibility of obtaining green light emission from a series of $In_xGa_{1-x}N$ QW thickness (L_W) and In composition (x). Examples include In composition (x) and QW thickness (L_W) of any of the following combinations, $x = 18\%$ and $L_W = 3.5$ nm (point A), $x = 25\%$ and $L_W = 2.2$ nm (point B), $x = 35\%$, and $L_W = 1.5$ nm (point C). We seek to determine which of the above combinations of the structural parameters will provide the most efficient high-intensity green light emission.

We determine the highest oscillator strength (F) value of the structure, which is considered proportional to the square overlap of the electron-hole wave functions ($F \propto |\langle \varphi_e | \varphi_{hh} \rangle|^2$). Radiative lifetime is inversely proportional to the square of the overlap of the electron and hole wave function integral as follows [33]:

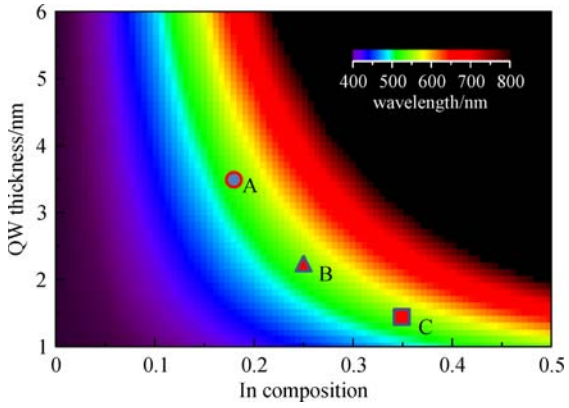

Fig. 1 Calculated wavelength as a function of In composition and QW thickness for InGaN/GaN system

$$\tau_{rad}^{-1} = \frac{nd^2E_0^3}{3\pi\varepsilon_0 h^4 c^3} \left| \int f_e f_h \mathrm{d}z \right|^2 = \frac{E_0^3}{A} \left| \int f_e f_h \mathrm{d}z \right|^2,$$

where d is the inter-band optical dipole of GaN, ε_0 is the permittivity of free space, h is Planck's constant, c is the speed of light, E_0 is the transition energy, and f_e and f_h are wave functions of electron and hole, respectively. The A value of 90 $eV^3 \cdot s$ was experimentally determined by Bretagnon et al. [34]. However, the relaxed in-plane lattice parameter of GaN, InN and AlN are different from each other ($a_{GaN} = 3.189$ Å, $a_{InN} = 3.538$ Å and $a_{AlN} = 3.113$ Å) [35,36]. Thus, by pseudomorphically growing InGaN/AlGaN layers on top of GaN as substrate layer, we must consider the polarization effect of InGaN and AlGaN layers because of strain.

The coefficients of piezoelectric polarization are significantly large in group-III nitrides [37,38]. Thus, the polar (*c*-plane) GaN/$In_xGa_{1-x}N$/$Al_yGa_{1-y}N$ growth structure experiences intense piezoelectric polarization effect because of GaN-InN lattice mismatch. Overall polarization (both spontaneous and piezoelectric) effects play a major role in electric field generation in all layers, such as barrier (GaN) electric field (E_b), well ($In_xGa_{1-x}N$) electric field, or internal electric field (E_W), and cap ($Al_yGa_{1-y}N$) electric field (E_C). The effects of internal electric field within well regions (E_W) will deform the band structure of the GaN/InGaN/AlGaN system and reduce the effective transition energy between different energy levels within the QWs. The band bending caused by internal electric field E_W and well thickness L_W will reduce the transition energy, which means the wavelength of emitted light will get red-shifted. This effect is known as quantum confined Stark effect (QCSE). The effect reduces the overlap of electron-hole wave-function, which is undesirable for any targeted intense wavelength emission. Thus, to obtain the oscillator strength (F) of the structure, we must first determine the induced electric fields of the heterostructure. The electric field of any layer of a superlattice can be determined by

following expression [39]:

$$E_j = \frac{\Sigma_i (P_i - P_j)\frac{L_i}{\varepsilon_i}}{\varepsilon_j \Sigma_i \frac{L_i}{\varepsilon_i}}, \quad (1)$$

where P_i and P_j are the total polarization of adjacent layer, ε_i and ε_j are permittivity of two adjacent layers.

The induced elastic strain energy per unit surface of the structure should also be considered by using the following expression:

$$E_{\mathrm{el}}(a_{\mathrm{eq}}) = \Sigma_{i=1}^{3} M_i L_i \Delta_i^2, \quad (2)$$

where M_i is the biaxial modulus, L_i is the layer thickness, $\Delta_i = (a_{\mathrm{eq}} - a_i)/a_i$ is the strain in the growth plane, a_i is the relaxed lattice parameter of each i layer (i corresponds to i = 1 = InGaN, i = 2 = AlGaN and i = 3 = GaN layer) and a_{eq} is the overall in-plane equilibrium lattice parameter of the entire GaN/InGaN/AlGaN heterostructure. This elastic strain energy value should be at the minimum to reduce the chance of defect formation within the structure because defects act as a non-radiative recombination center.

Biaxial modulus M_i and relaxed lattice parameter a_i of epilayers depend on the particular composition values of the layer. The biaxial modulus of $In_xGa_{1-x}N$ layer should be calculated based on the following equation:

$$M_{\mathrm{In_xGa_{1-x}N}} = \left(c_{11}(x) + c_{12}(x) - \frac{2c_{13}(x)^2}{c_{33}(x)}\right), \quad (3)$$

where c_{jk} are the elastic stiffness constants of $In_xGa_{1-x}N$ layer and their values can be obtained using Vegard's law as

$$c_{jk}(x) = x c_{jk}(\mathrm{InN}) + (1-x) c_{jk}(\mathrm{GaN}). \quad (4)$$

Here, $c_{jk}(\mathrm{InN})$ and $c_{jk}(\mathrm{GaN})$ values are considered from Nikolaev et al. [40]. Similar equations should be considered for $Al_yGa_{1-y}N$ layer. In this work, we did not consider the bowing parameter (b = 0) when calculating the band gap energy to avoid further complexity. We may also consider that E_{el} is the minimum when $\frac{\mathrm{d}E_{\mathrm{el}}}{\mathrm{d}a_{\mathrm{eq}}} = 0$, and the in-plane equilibrium lattice parameter of the whole structure can be expressed as

$$a_{\mathrm{eq}} = \frac{\Sigma_{i=1}^{3}(M_i L_i \prod_{j \neq i} a_j)}{\Sigma_{i=1}^{3}(M_i L_i \prod_{j \neq i} a_j^2)} \prod_{i-1}^{3} a_i. \quad (5)$$

This study considered different parameters of the structure, such as the In composition (x) and layer thickness (L_{W}) of $In_xGa_{1-x}N$ QW region, Al composition (y) and layer thickness (L_{C}) of $Al_yGa_{1-y}N$ cap layer while keeping GaN barrier layer thickness (L_{b}) at 12 nm. The electric field of different layers is then calculated using Eq. (1). Then, using the different layers' electric field values along with the structural parameters, we attempted to simulate and identify the transition energy (emission wavelength), oscillator strength, elastic strain energy per surface, and in-plane equilibrium lattice parameter a_{eq} values of the structure.

3 Simulation process

To obtain green light (525–565 nm) emission, we initially chose three models that consider the sample (as shown schematically in Fig. 2) parameters shown in Table 1. QW thickness and In composition values were taken to match those of the points from Fig. 1. The Al composition of each model are initially taken arbitrarily to 50% and AlGaN cap layer thickness (L_{C}) values to make the one period length in between 14.5 and 16.5 nm.

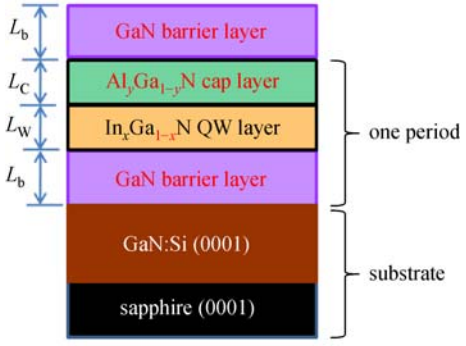

Fig. 2 Schematic diagram of the simulated structure

Oscillator strength (F) and in-plane equilibrium lattice parameter (a_{eq}) should be identified to determine the best structural parameters for high-intensity green emission. To identify the highest possible oscillator strength and the lowest elastic strain energy values, we analyzed the structure by varying each parameter individually while keeping all other parameters fixed. The following steps are then considered.

Step 1: The Al composition (y) of $Al_yGa_{1-y}N$ cap layer is varied while keeping other parameters fixed to obtain the best value of Al composition.

Step 2: The In composition (x) of $In_xGa_{1-x}N$ QW layer is varied while keeping the best value of Al composition obtained in Step 1 and other parameters fixed.

Step 3: The $In_xGa_{1-x}N$ QW thickness (L_{W}) value is varied while keeping the best values of Al and In compositions obtained in Step 1 and 2 and other parameters fixed.

Step 4: The $Al_yGa_{1-y}N$ cap layer thickness (L_{C}) value is varied, while keeping all other best values of parameters obtained from the previous steps.

Table 1 Initial structural parameters of the models for green light emission

	barrier length, L_b/nm	In composition (x)/%	$In_xGa_{1-x}N$ QW thickness, L_W/nm	Al composition (y)/%	cap layer ($Al_yGa_{1-y}N$) thickness, L_C/nm
Model 1	12	25	2.2	50	1.2
Model 2	12	18	3.5	50	1.5
Model 3	12	35	1.5	50	1.0

4 Result and discussion

4.1 Model 1

The structural parameters for Model 1 are provided in Table 2 where Al compositions are varied. The results obtained for Model 1 of the simulation process are discussed. First, we calculated different layer electric field values for each Al composition using Eq. (1). Then, we simulated the band diagram of the structure for each change. Figure 3 shows the band diagram of Model 1, wherein structural parameters are taken from Table 1 and electric field values are given as: barrier electric field, E_b = 227.9 kV/cm, InGaN QW electric field, E_W = 4158.1 kV/cm and AlGaN cap layer electric field, E_C = 5343.7 kV/cm. We can easily identify the band bending phenomenon in the figure because of different values of layers' field and the green line in the figure that indicates the simulated electron wave function within the QW region of the structure.

The band diagram allows us to determine the transition energy and oscillator strength values. We calculated the elastic strain energy (E_{el}) and overall in-plane equilibrium lattice parameter (a_{eq}) using Eqs. (2) and (5), respectively. The results are presented in Table 3.

Table 3 shows that the best result is found when Al composition (y) is 70% because it has high oscillator strength ($F = 1.49 \times 10^{-1}$) at wavelength of 529 nm and low in-plane equilibrium lattice parameter ($a_{eq} \cong 3.219$Å) value, which is slightly mismatched to GaN lattice parameter ($a_{GaN} \cong 3.189$Å) of 0.94%. For Al compositions (y) higher than 70%, the observed oscillator strength value becomes low, whereas lower Al composition ($y < 70\%$) increases oscillator strength and in-plane equilibrium lattice parameter. However, increased value of in-plane equilibrium lattice parameter is undesirable. This finding is attributed to the facts that the higher in-plane equilibrium lattice parameter value relates to increased chance of defect formation within the structure; these defects act as non-radiating recombination centers for electron-hole pairs. Thus, emitted light intensity will become degraded for structures with lower ($< 70\%$) Al composition cap layers.

The variation of In composition (x) in $In_xGa_{1-x}N$ QW was examined. In composition (x) was varied to a maximum of $\pm 3\%$ to that of initial considered value (25%) to determine its effect on in-plane equilibrium lattice parameter, oscillator strength, and emission wavelength values. This method is adopted to keep other parameters fixed and Al composition is fixed at 70%, as obtained Step 1. The obtained results are shown in Table 4.

Table 4 indicates a slight decrease of In composition (x) at 25% will cause the emission wavelength to blue shift from 529 nm to 509 nm, which is undesirable. However, a slight increase of In composition (x) red shifts the emission to facilitate green light emission. Oscillator strength (F) decreases and in-plane equilibrium lattice parameter (a_{eq}) increases, which increase the chance of dislocation, thereby decreasing light intensity. Thus, In composition of 25% is the best parameter as it provides low in-plane equilibrium lattice parameter ($a_{eq} \cong 3.219$Å) and high oscillator strength ($F = 1.49 \times 10^{-1}$) in the wavelength of green light emission (525–565 nm).

The thickness variation of InGaN QW was also examined by simulating the structure and maintaining the compositions of Al and In compositions fixed at 70% and 25%. The result obtained from such simulation for emission wavelength, in-plane equilibrium lattice parameter, and oscillator strength is given in Table 5.

The result in Table 5 shows that decreased QW thickness improved the parameters, but emission wavelength blue shifts from green emission. Thus, we cannot excessively decrease QW thickness. However, a slight increase in QW thickness value (from 2.2 to 2.3 nm) facilitates the central emission peak (539 nm) of green light spectrum (525–565 nm), but the lattice parameter of in-plane equilibrium and oscillation strength was slightly degraded. Thus, we selected QW thickness of 2.3 nm to obtain an emission wavelength of 539 nm, in-plane equilibrium lattice parameter (a_{eq}), and oscillator strength (F) of about 3.220 Å and 1.21×10^{-1}.

In Step 4, the variation of $Al_{0.7}Ga_{0.3}N$ cap layer

Table 2 Structural parameters for Model 1 as in Step 1 of the simulation process

type	barrier length, L_b/nm	In composition (x)/%	QW thickness, L_W/nm	Al composition (y)/%	cap layer ($Al_yGa_{1-y}N$) thickness, L_C/nm
Model 1	12	25	2.2	variable	1.2

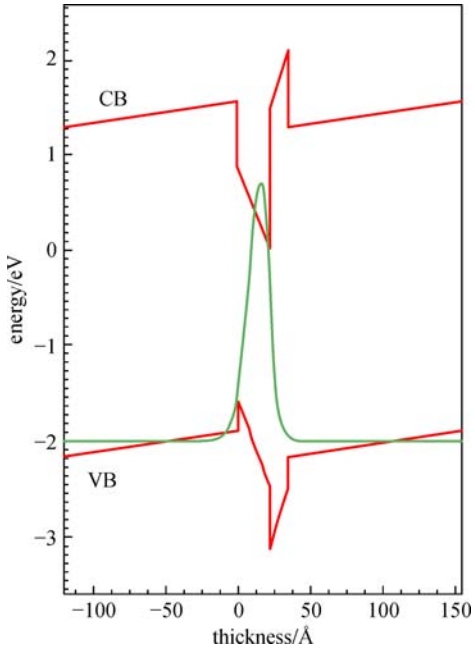

Fig. 3 Energy band diagram of Model 1, wherein the structural parameters are taken from Table 1. The red lines show the valance band (VB) and conduction band (CB) and the green line is the electron wave function of the GaN/$In_{0.25}Ga_{0.75}N$/$Al_{0.50}Ga_{0.50}N$/GaN structure

thickness (L_C) was examined. The results are shown in Table 6. Cap layer thickness L_C of 1.3 nm provides the best results, but a slight increase in L_C lowers the oscillator strength from 1.18×10^{-1} to 1.14×10^{-1}. A slight decrease in L_C (see Table 6) increases oscillator strength (F) value and in-plane equilibrium lattice parameter (a_{eq}), which will increase the chance of generating dislocation in the structure.

4.2 Comparison

The best parameters for Models 2 and 3 (as described in Table 1) were also identified and summarized in Table 7. A comparison of the three models shows that each model will provide green light, but the intensity of Model 2 will be low because oscillator strength (F) is the lowest ($F = 1.05 \times 10^{-2}$); however, the in-plane equilibrium lattice parameter is lowest ($a_{eq} \cong 3.217$Å), which suggest the least possible defects in the structure. A comparison between Model 1 and 3 suggests that Model 1 is slightly better because the in-plane equilibrium lattice parameter (a_{eq}) is slightly lower in value than that of Model 3 (Table 7). This finding suggests that the change in defect generation is low for Model 1 because the strain value is lower than that of Model 3 (for Model 1, strain is $\Delta = (3.2182-3.189)/3.189 = 9.18 \times 10^{-3}$ and that for Model

Table 3 Variation of in-plane equilibrium lattice parameter, oscillator strength, and emission wavelength as a function of Al composition

Al composition(y)/%	in-plane equilibrium lattice parameter, a_{eq}/Å	oscillator strength, F	wavelength/nm
50	3.226	1.54×10^{-1}	527
60	3.222	1.53×10^{-1}	528
70	**3.219**	$\mathbf{1.49\times10^{-1}}$	**529**
78	3.216	1.46×10^{-1}	530

Table 4 Variation of in-plane equilibrium lattice parameter, oscillator strength and emission wavelength as a function of In composition

In composition(x)/%	in-plane equilibrium lattice parameter, a_{eq}/Å	oscillator strength, F	wavelength/nm
23	3.215	1.67×10^{-1}	509
24	3.217	1.58×10^{-1}	519
25	**3.219**	$\mathbf{1.49\times10^{-1}}$	**529**
26	3.221	1.41×10^{-1}	539
27	3.223	1.34×10^{-1}	550
28	3.225	1.27×10^{-1}	561

Table 5 Variation of in-plane equilibrium lattice parameter, oscillator strength and emission wavelength as a function of QW thickness

QW thickness, L_W/nm	in-plane equilibrium lattice parameter, a_{eq}/Å	oscillator strength, F	wavelength/nm
2	3.216	2.19×10^{-1}	511
2.1	3.217	1.82×10^{-1}	520
2.2	3.219	1.49×10^{-1}	529
2.3	**3.220**	$\mathbf{1.21\times10^{-1}}$	**539**
2.35	3.221	8.35×10^{-2}	548

Table 6 Variation of in-plane equilibrium lattice parameter, oscillator strength and emission wavelength as a function of AlGaN cap layer thickness

cap layer thickness, L_C/nm	in-plane equilibrium lattice parameter, a_{eq}/Å	oscillator strength, F	wavelength/nm
1.2	3.220	1.21×10^{-1}	539
1.3	**3.218**	$\mathbf{1.18\times10^{-1}}$	**540**
1.4	3.215	1.14×10^{-1}	541

Table 7 Summary of the three models

type	barrier length, L_b/nm	In composition (x)/%	QW thickness, L_W/nm	Al composition (y)/%	cap layer ($Al_yGa_{1-y}N$) thickness, L_C/nm	emission wavelength, λ/nm	oscillator strength, F	in-plane equilibrium lattice parameter, a_{eq}/Å
Model 1	12	25	2.3	70	1.3	540	1.18×10^{-1}	3.218
Model 2	12	18	3.6	40	1.8	542	1.05×10^{-2}	3.217
Model 3	12	35	1.6	67	1.2	548	3.18×10^{-1}	3.224

3 is $\Delta = (3.22498 - 3.189)/3.189 = 11.28 \times 10^{-3}$). However, oscillator strength is slightly low.

5 Conclusion

We simulated and analyzed $GaN/In_xGa_{1-x}N/Al_yGa_{1-y}N$ heterostructures to identify the best structural parameters for high-intensity green and yellowish green light (525–565 nm) emissions. We determine the appropriate structure that provides the highest oscillator strength (F) and lowest elastic strain energy values. A comparison of the data of three models (Table 7) shows the structure of Model 1 for $In_xGa_{1-x}N$ QW, In composition (x = 25%) and thickness (L_W = 2.3 nm), $Al_yGa_{1-y}N$ cap layer for Al composition (y = 70%) with a cap layer thickness of L_C = 1.3 nm. This value provides a relatively high oscillator strength (F) value of 1.18×10^{-1} and low in-plane equilibrium lattice parameter (a_{eq}) of 3.218 Å. Thus, the structure of Model 1 will have the least structural defects and will provide green light with higher intensity than the other two models (i.e., Models 2 and 3).

Acknowledgements The authors thank Dr. Benjamin Damilano and Mr. Philippe Vennéguès, Centre de Recherche sur l'H´et´ero-Epitaxie et ses Applications (CRHEA), Centre National de la Recherche Scientifique (CNRS), Valbonne 06560, France for their support.

References

1. Nakamura S, Fasol G. The Blue Laser Diode. Berlin: Springer, 1997
2. Krames M R, Shchekin O B, Mueller-Mach R, Mueller G O, Zhou L, Harbers G, Craford M G. Status and future of high-power light-emitting diodes for solid-state lighting. Journal of Display Technology, 2007, 3(2): 160–175
3. Narukawa Y, Ichikawa M, Sanga D, Sano M, Mukai T. White light emitting diodes with super-high luminous efficacy. Journal of Physics D, Applied Physics, 2010, 43(35): 354002
4. Crawford M H. LEDs for solid-state lighting: performance challenges and recent advances. IEEE Journal of Selected Topics in Quantum Electronics, 2009, 15(4): 1028–1040
5. Langer T, Kruse A, Ketzer FA, Schwiegel A, Hoffmann L, Jönen H, Bremers H, Rossow U, Hangleiter A. Origin of the "green gap": increasing nonradiative recombination in indium-rich GaInN/GaN quantum well structures. Physica Status Solidi (C), 2011, 8(7–8): 2170–2172
6. Zhu M, You S, Detchprohm T, Paskova T, Preble E A, Wetzel C. Various misfit dislocations in green and yellow GaInN/GaN light emitting diodes. Physica Status Solidi (A), 2010, 207(6): 1305–1308
7. Tessarek C, Figge S, Aschenbrenner T, Bley S, Rosenauer A, Seyfried M, Kalden J, Sebald K, Gutowski J, Hommel D. Strong phase separation of strained $In_xGa_{1-x}N$ layers due to spinodal and binodal decomposition: Formation of stable quantum dots. Physical Review B: Condensed Matter and Materials Physics, 2011, 83(11): 115316
8. Qi Y D, Liang H, Wang D, Lu Z D, Tang W, Lau K M. Comparison of blue and green InGaN/GaN multiple-quantum-well light-emitting diodes grown by metalorganic vapor phase epitaxy. Applied Physics Letters, 2005, 86(10): 101903
9. Na J H, Taylor R A, Lee K H, Wang T, Tahraoui A, Parbrook P, Fox A M, Yi S N, Park Y S, Choi J W, Lee J S. Dependence of carrier localization in InGaN/GaN multiple-quantum wells on well thickness. Applied Physics Letters, 2006, 89(25): 253120
10. Sato H, Tyagi A, Zhong H, Fellows N, Chung R B, Saito M, Fujito K, Speck J S, DenBaars S P, Nakamura S. High power and high efficiency green light emitting diode on free-standing semipolar (112) bulk GaN substrate. Physica Status Solidi (RRL) – Rapid Research Letters, 2007, 1(4): 162–164
11. Schwarz U T, Kneissl M. Nitride emitters go nonpolar. Physica Status Solidi (RRL) – Rapid Research Letters, 2007, 1(3): A44–A46
12. El-Masry N A, Piner E L, Liu S X, Bedair S M. Phase separation in InGaN grown by metalorganic chemical vapor deposition. Applied Physics Letters, 1998, 72(1): 40–42
13. Pristovsek M, Kadir A, Meissner C, Schwaner T, Leyer M, Kneissl M. Surface transition induced island formation on thin strained InGaN layers on GaN (0001) in metal-organic vapour phase epitaxy. Journal of Applied Physics, 2011, 110(7): 073527
14. Adachi M. InGaN based green laser diodes on semipolar GaN

substrate. Japanese Journal of Applied Physics, 2014, 53(10): 100207
15. Koslow I L, Hardy M T, Shan Hsu P, Dang P Y, Wu F, Romanov A, Wu Y R, Young E C, Nakamura S, Speck J S, DenBaars S P. Performance and polarization effects in (112) long wavelength light emitting diodes grown on stress relaxed InGaN buffer layers. Applied Physics Letters, 2012, 101(12): 121106
16. Strauß U, Avramescu A, Lermer T, Queren D, Gomez-Iglesias A, Eichler C, Müller J, Brüderl G, Lutgen S. Pros and cons of green InGaN laser on c-plane GaN. Physica Status Solidi (B), 2011, 248 (3): 652–657
17. Arif R A, Ee Y K, Tansu N. Polarization engineering via staggered InGaN quantum wells for radiative efficiency enhancement of light emitting diodes. Applied Physics Letters, 2007, 91(9): 091110
18. Zhao H, Tansu N. Optical gain characteristics of staggered InGaN quantum wells lasers. Journal of Applied Physics, 2010, 107(11): 113110
19. Han S H, Cho C Y, Lee S J, Park T Y, Kim T H, Park S H, Won Kang S, Won Kim J, Kim Y C, Park S J. Effect of Mg doping in the barrier of InGaN/GaN multiple quantum well on optical power of light-emitting diodes. Applied Physics Letters, 2010, 96(5): 051113
20. Shioda T, Yoshida H, Tachibana K, Sugiyama N, Nunoue S. Enhanced light output power of green LEDs employing AlGaN interlayer in InGaN/GaN MQW structure on sapphire (0001) substrate. Physica Status Solidi (A), 2012, 209(3): 473–476
21. Lefebvre P, Taliercio T, Morel A, Allègre J, Gallart M, Gil B, Mathieu H, Damilano B, Grandjean N, Massies J. Effects of GaAlN barriers and of dimensionality on optical recombination processes in InGaN quantum wells and quantum boxes. Applied Physics Letters, 2001, 78(11): 1538–1540
22. Lu H M, Chen G X. Design strategies for mitigating the influence of polarization effects on GaN-based multiple quantum well light-emitting diodes. Journal of Applied Physics, 2011, 109(9): 093102
23. Zhao H, Arif R A, Ee Y K, Tansu N. Self-consistent analysis of strain-compensated InGaN-AlGaN quantum wells for lasers and light-emitting diodes. IEEE Journal of Quantum Electronics, 2009, 45(1): 66–78
24. Tsai C L, Fan G C, Lee Y S. Effects of strain-compensated AlGaN/InGaN superlattice barriers on the optical properties of InGaN light-emitting diodes. Applied Physics A, Materials Science & Processing, 2011, 104(1): 319–323
25. Koleske D D, Fischer A J, Bryant B N, Kotula P G, Wierer J J. On the increased efficiency in InGaN-based multiple quantum wells emitting at 530–590 nm with AlGaN interlayers. Journal of Crystal Growth, 2015, 415: 57–64
26. Saito S, Hashimoto R, Hwang J, Nunoue S. InGaN light-emitting diodes on c-face sapphire substrates in green gap spectral range. Applied Physics Express, 2013, 6(11): 111004
27. Hwang J I, Hashimoto R, Saito S, Nunoue S. Development of InGaN-based red LED grown on (0001) polar surface. Applied Physics Express, 2014, 7(7): 071003
28. Doi T, Honda Y, Yamaguchi M, Amano H. Strain-compensated effect on the growth of InGaN/AlGaN multi-quantum well by metalorganic vapor phase epitaxy. Japanese Journal of Applied Physics, 2013, 52(8S): 08JB14
29. Damilano B, Kim-Chauveau H, Frayssinet E, Brault J, Hussain S, Lekhal K, Vennéguès P, Mierry P D, Massies J. Metal organic vapor phase epitaxy of monolithic two-color light-emitting diodes using an InGaN-based light converter. Applied Physics Express, 2013, 6(9): 092105
30. Lekhal K, Damilano B, Ngo H T, Rosales D, Mierry P D, Hussain S, Vennéguès P, Gil B. Strain-compensated (Ga,In)N/(Al,Ga)N/GaN multiple quantum wells for improved yellow/amber light emission. Applied Physics Letters, 2015, 106(14): 142101
31. Damilano B, Gil B. Yellow–red emission from (Ga,In)N heterostructures. Journal of Physics D, Applied Physics, 2015, 48(40): 403001
32. Lekhal K, Hussain S, Mierry P D, Vennéguès P, Nemoz M, Chauveau J M, Damilano B. Optimized In composition and quantum well thickness for yellow-emitting (Ga,In)N/GaN multiple quantum wells. Journal of Crystal Growth, 2016, 434: 25–29
33. Thränhardt A, Ell C, Khitrova G, Gibbs H M. Relation between dipole moment and radiative lifetime in interface fluctuation quantum dots. Physical Review B: Condensed Matter and Materials Physics, 2002, 65(3): 035327
34. Bretagnon T, Lefebvre P, Valvin P, Bardoux R, Guillet T, Taliercio T, Gil B, Grandjean N, Semond F, Damilano B, Dussaigne A, Massies J. Radiative lifetime of a single electron-hole pair in GaN/AlN quantum dots. Physical Review B: Condensed Matter and Materials Physics, 2006, 73(11): 113304
35. Narukawa Y, Sano M, Ichikawa M, Minato S, Sakamoto T, Yamada T, Mukai T. Improvement of luminous efficiency in white light emitting diodes by reducing a forward-bias voltage. Japanese Journal of Applied Physics, 2007, 46(40): L963–L965
36. Meneghini M, Tazzoli A, Mura G, Meneghesso G, Zanoni E. A review on the physical mechanisms that limit the reliability of GaN-based LEDs. IEEE Transactions on Electron Devices, 2010, 57(1): 108–118
37. Bernardini F, Fiorentini V, Vanderbilt D. Spontaneous polarization and piezoelectric constants of III-V nitrides. Physical Review B: Condensed Matter and Materials Physics, 1997, 56(16): R10024–R10027
38. Bernardini F, Fiorentini V. First-principles calculation of the piezoelectric tensor d of III–V nitrides. Applied Physics Letters, 2002, 80(22): 4145–4147
39. Bernardini F, Fiorentini V. Polarization fields in nitride nanostructures: 10 points to think about. Applied Surface Science, 2000, 166(1–4): 23–29
40. Nikolaev V V, Portnoi M E, Eliashevich I. Photon recycling white light emitting diode based on InGaN multiple quantum well heterostructure. Physica Status Solidi (A), 2001, 183(1): 177–182

Sakhawat Hussain received his B.Sc. and M.Sc. degrees from University of Dhaka, Bangladesh in 2007 and 2008, respectively. In 2014, he successfully completed his Ph.D. in Physics (Optoelectronics) from the University of Nice-Sophia Antipolis (UNS), France. During his Ph.D. studies, he worked at the research laboratory of "Centre de Recherche sur l'Hétéro-Epitaxie

et ses Applications (CRHEA), France" under the opto-electronics group. His research focus was on structural and optical characterization of GaN/InGaN/AlGaN heterostructures as light emitting diodes for yellow-green light emission. His research interests are in group III-Nitride semiconductor materials and their applications. At present, he is working as an Assistant Professor at the Department of Electrical and Electronic Engineering, University of Dhaka, Bangladesh.

Tasnim Zerin earned her B.Sc. degree from the Department of Applied Physics, Electronics and Communication Engineering in the University of Dhaka in 2013. She completed her M.Sc. degree from the same university in 2015. Her research interests are centered on material science and applied physics. She is currently looking forward to her Ph.D. study on any relevant topic of her research interest.

Md. Ashik Khan received his M.Sc. degree in Electrical and Electronic Engineering from the University of Dhaka, Bangladesh in 2015. He completed his B.Sc. degree from the same university in 2013. His research interests are on optics related fields such as optoelectronics, optical communications, and lasers. At present, Mr. Khan is serving as a government employee at the Bangladesh Civil Service. He is looking forward to his Ph.D. study from a top university.